Application Note

Single Stage SRC-DAB Design for Low Voltage Residential ESS Application

Will Tai, Guangzhi Cui

ABSTRACT

The growing interest towards high efficiency, wide input/output range bidirectional DC-DC converters for energy storage systems (ESS) applications attracts more research of different topologies and control methods. This document focuses on the series resonant dual active bridge (SR-DAB) converter. The design considerations and optimization control scheme of the SR-DAB converter is discussed, which includes the reactive power optimization, zero voltage detection method and turn off current optimization. Furthermore, a 3.6kW SR-DAB prototype is built to evaluate performance.

Trademarks

All trademarks are the property of their respective owners.

Copyright © 2026 Texas Instruments Incorporated

1 Introduction

With the maturity of Lithium-ion battery technologies 1 and the exponential increase of the numbers of electric vehicles and energy storage systems 2, efficient power conversion interface becomes more and more important to those battery charger applications. Four isolated DC-DC converter topologies, LLC series resonant converters (LLC) [3], CLLLC series resonant converters (CLLLC) 4 , dual active bridge converter (DAB) and series resonant dual active bridge converter (SR-DAB) 5, 6 are either widely applied in today's ESS applications or are of interest because of advantageous characteristics in certain applications. Figure 1-1 illustrates these four topologies of options. Key characteristics of these four topologies are summarized in Figure 1-2. Based on the summary in the table, both LLC and CLLLC use frequency modulation control (FMC) and the energy stored in the magnetizing inductor (L_m) of the transformer to achieve zero voltage switching (ZVS) of the primary side switches. Therefore, both LLC and CLLLC are able to achieve full range ZVS regardless of the load current condition. However, most battery charger applications, such as ESS, usually need wide gain range. It is difficult for LLC/CLLLC to cover such wide gain range while remaining a high efficiency. DAB using phase-shift control (PSC) instead of FMC which allows faster and uninterrupted power transition between forward and reverse power flow, besides, it allows wider voltage adjust range. However, DAB uses the energy stored in the series inductor to achieve primary side switches' ZVS, the primary side switches ZVS are load current dependent. Moreover, the turn-off current in low voltage side increased dramatically with power level increasing if the voltage gain is far away from one under single-phase shift control, which leads to high turn-off loss. By inserting a series resonant tank in the DAB converter, it forms the SR-DAB. This topology keeps the wide voltage adjust range feature and due to the resonance feature, the inductor current in SR-DAB is almost sinusoidal, which will lead to smaller turn off current compared with DAB. In addition, the SR-DAB normally operates higher than the resonant frequency, which supplies the necessary condition to realize ZVS. Therefore, SR-DAB is a better choice for ESS applications. Table 1-1 shows the key system specifications targeting a popular 3.6kW ESS application. The next section discusses the key design considerations and optimization control scheme of SR-DAB in ESS applications. A SR-DAB prototype has been made to verify the analysis in final section.

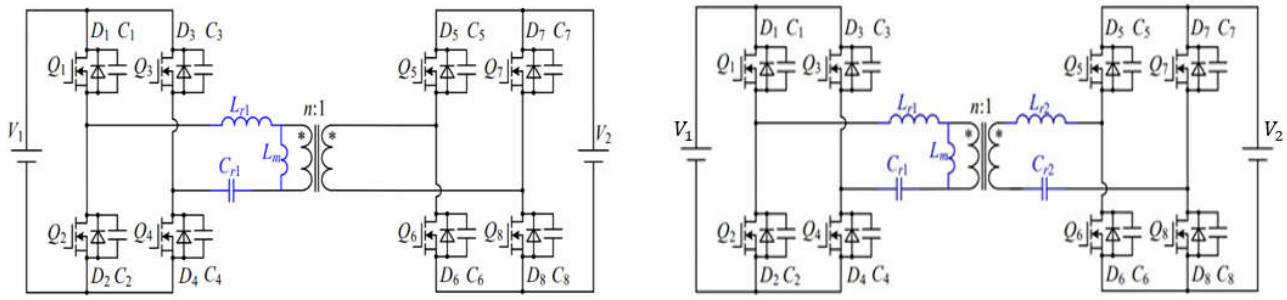
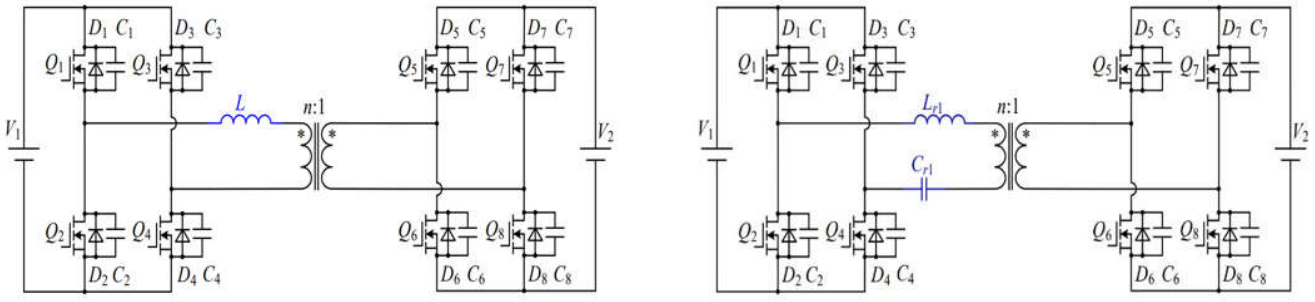


Figure 1-1. Topology Diagram (a) LLC. (b) CLLLC. (c) DAB. (d) SR-DAB



Copyright © 2026 Texas Instruments Incorporated

LLC	CLLLC	DAB	DABSRC
Benefits: • Full range ZVS • Low cost • Simple control method Challenges: • Narrow voltage adjust range • Gain below 1 in reverse mode • Slow dynamic response and bidirectional power transition	Benefits: • Full range ZVS • Symmetric gain features • Simple control method Challenges: • Narrow voltage adjust range • High cost due to secondary resonant tank • Slow dynamic response and bidirectional power transition	Benefits: • Wide voltage adjust range • Lowest cost • Fast dynamic response and bidirectional power transition Challenges: • Low efficiency and high turn off current with single phase control • Hard to realize ZVS at light load • Need complex control method to optimize the performance	Benefits: • Wide voltage adjust range • Wider ZVS range than DAB • Lower RMS current and turn off current than DAB Challenges: • Low efficiency with single phase shift control • Need complex control method to optimize the performance

Figure 1-2. Summary of Different Topologies

Table 1-1. System Specifications

Rated Power (P)	Input Voltage (V_{IN})	Output Voltage (V_O)
3.6kW	350V to 550V	40V to 60V

Copyright © 2026 Texas Instruments Incorporated

2 Detailed Description

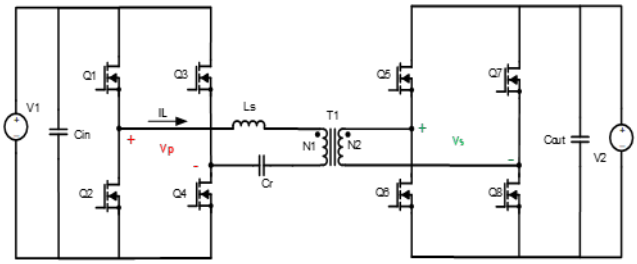


Figure 2-1. Schematic of SR-DAB

The schematic of SR-DAB is in Figure 2-1 The switches Q1 –Q4 form the primary side full bridge and are modulated to generate Vp. The secondary side full bridge of the converter consists of Q5 –Q8, which are modulated to generate a voltage Vs. In this phenomenon, there is higher turn off loss if the turn off current in low voltage side is high. Therefore, knowing how to minimize the turn-off current in low voltage side is important. In this section, a turn-off current and reactive power optimization method is proposed to improve system efficiency.

3 Achieving Minimum Turn Off Current in Low Voltage Side

To optimize the performance of the SR-DAB design, the control strategy is based on Multiple-Degrees-of-Freedom Modulation, which is multiple phase shift with a variable frequency modulation. Figure 3-1 shows the typical waveform when the voltage gain M<1 (M is defined as $N_1 \times V_2/N_2 \times V_1$). In this case, the topology operates in EPS (extended phase shift) modulation mode, there is an inner phase shift angle Øa on the primary side, and as a result, the measured voltage Vp of the primary side bridge is a three-level square wave, while the secondary side voltage Vs is a two-phase square wave. Additionally, there is also an external phase shift angle Øb between the primary and secondary sides. By performing FHA analysis on Vp and Vs, the user can obtain the expressions of Vp and Vs after normalization:

$$V_{p_pu}(t) = \frac{4 \cdot cos\emptyset a}{\pi} sin\omega t \quad (1)$$

$$V_{s_pu}(t) = \frac{4 \cdot M}{\pi} sin(\omega t - \emptyset b) \quad (2)$$

Figure 3-2 shows the simplified schematic of LC series resonant tank of SR-DAB. Operating the switching frequency fs higher than the resonant frequency fr makes the resonant tank located in the inductive region. Therefore, the resonant voltage V_{res} is 90° ahead of the current iL. Based on this constraint, achieving the minimum turn-off current on the low-voltage side, that is iL (Øb) = 0. The constraint equation is given as Equation 3

$$\mathrm{iL}(\emptyset b) = V_{res_pu}\left(\frac{\pi}{2} + \emptyset b\right)/\mathrm{Zr} = 0 \quad (3)$$

$$V_{res_pu}\left(\frac{\pi}{2} + \emptyset b\right) = V_{p_pu}\left(\frac{\pi}{2} + \emptyset b\right) - V_{s_pu}\left(\frac{\pi}{2} + \emptyset b\right) = 0 \quad (4)$$

Where Zr is the impedance of the resonant tank. By solving above equations, Equation 5 is obtained.

$$cos(\emptyset a) \cdot cos(\emptyset b) = M(M < 1) \quad (5)$$

Figure 3-1 shows the typical waveforms when voltage gain M≥1. In this case, the topology also operates in EPS modulation mode. There is an inner phase shift angle Øc on the secondary side, hence the measured voltage Vs of secondary side bridge is a three-level square wave, while the primary side voltage Vp is a two-phase square wave. Additionally, there is also an external phase shift angle Øb between the primary and secondary sides. Similarly, by using the FHA analysis, the user can obtain the expressions of Vp and Vs after normalization:

$$V_{p_pu}(t) = \frac{4}{\pi} sin\omega t \quad (6)$$

Copyright © 2026 Texas Instruments Incorporated

$$V_{s_pu}(t) = \frac{4 \cdot M \cdot cos\emptyset c}{\pi} sin(\omega t - \emptyset b) \quad (7)$$

Note that only one leg (leading leg) in secondary side can achieve minimum turn-off current because of the inner phase shift angle Øc on the secondary side. And this minimum turn-off current is achieved when iL (Øb – Øc) = 0. The constraint equation is shown as Equation 8 and Equation 9

$$\mathrm{iL}(\emptyset b - \emptyset c) = V_{res_{pu}}\left(\frac{\pi}{2} + \emptyset b - \emptyset c\right)/\mathrm{Zr} = 0 \quad (8)$$

$$V_{res_{pu}}\left(\frac{\pi}{2} + \emptyset b - \emptyset c\right) \quad (9)$$

By solving previous equations, the user obtains Equation 10

$$cos(\emptyset c) \cdot cos(\emptyset c) \cdot M = \cos(\emptyset b - \emptyset c)(M \geq 1) \quad (10)$$

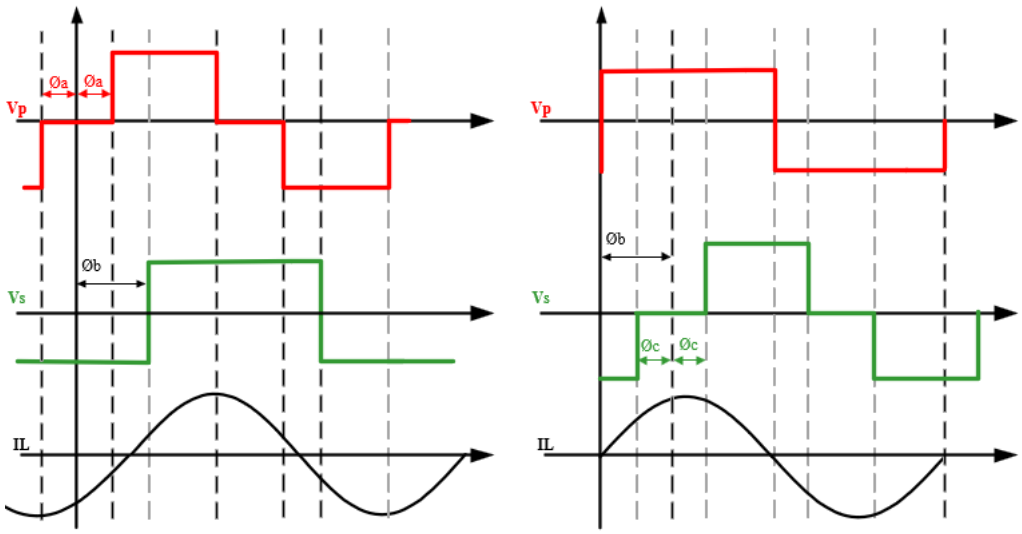


Figure 3-1. Typical Waveforms of SR-DAB (a) M < 1 (b) M ≥ 1

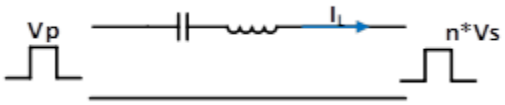


Figure 3-2. Simplified Schematic of the Resonant Tank

Copyright © 2026 Texas Instruments Incorporated

4 Minimum Reactive Power

Figure 4-1 shows a waveform of the primary side that generates reactive power. At this point, the voltage Vp is positive, but the resonant tank current is negative, resulting in negative instantaneous power. This means that power is not be transferred to the secondary side, and this energy circulates internally within the primary side, causing additional losses. Preferably, the reactive power in this part is zero, which means the region where Vp is positive, and current in the resonant tank is also positive. Therefore, to realize zero reactive power when M < 1, the user only needs to make $\emptyset a = \emptyset b$ as shown in Figure 4-1. Similarly, for the case when M ≥ 1, calculate $\emptyset c = \emptyset b$ to realize zero reactive power. Referring to the analysis in Figure 4-1, the constraint of Equation 5 and Equation 10 are obtained. Based on this, derive the expression for the two-phase angles when M < 1 and M ≥ 1, which are:

$$\emptyset a = \emptyset b = arcsin(\sqrt{1 - M})(\mathrm{M} < 1) \tag{11}$$

$$\emptyset c = \emptyset b = arcsin\left(\sqrt{1 - \frac{1}{M}}\right)\left(\mathrm{M} \geq 1\right) \tag{12}$$

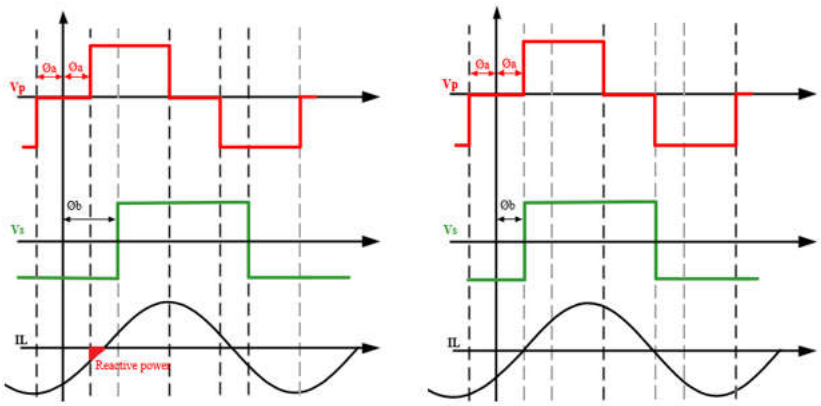


Figure 4-1. Reactive Power Waveforms (A) With Reactive Power (B) Without Reactive Power

Copyright © 2026 Texas Instruments Incorporated

5 Control Scheme of SR-DAB Combined With ZVD

The control block diagram is shown in Figure 5-1. A variable frequency with EPS modulation is used in the design. The switching frequency fs is determined by the feedback loop to regulate the output current, while using the phase angles calculated above to optimize the reactive power and turn-off current. It is worth noting that the analysis in the above sections only considers the zero turn-off current and zero reactive power, but does not consider the margin required to achieve ZVS, particularly for the primary-side devices. In practice, a certain amount of negative current is required to help achieve ZVS, as shown in Figure 5-2. Therefore, the converter cannot operate under completely zero reactive power conditions and the reactive power must be appropriately provided especially on light load conditions. Typically, for such cases, fine adjustments can be made to the phase angle based on experience, but there is an issue regarding the amount of reactive power that is supplied to achieve ZVS. Providing too many results in a larger turn-off current and higher circulating current, while providing a small amount can make it unable to fully achieve ZVS.

In fact, the problem becomes how to determine the current required to achieve ZVS. Actually, use time-domain analysis to obtain the corresponding current magnitude and then calculate the phase-shift angle. However, this method is affected by circuit parameters, which cannot remain constant, so the accuracy of this method is also impacted. This article proposes a method that uses the gallium nitride (GaN) with the integrated zero-voltage detection (ZVD) function to achieve adaptive adjustment of the phase-shift angle, thereby helping realize ZVS in the primary side. This ZVD feature provides a pulse output when ZVS is realized, which helps optimize performance of GaN devices. Based on this, a simple logic is implemented: reducing the reactive power (used to supply ZVS current) when the ZVD signal is received; when the ZVD signal is lost, increasing the reactive power again. By using this method, the current for achieving ZVS can always remain at an optimal level while verifying ZVS implementation without increasing additional losses, which helps optimize the efficiency. The complete ZVD-based control block diagram is shown in Figure 5-3.

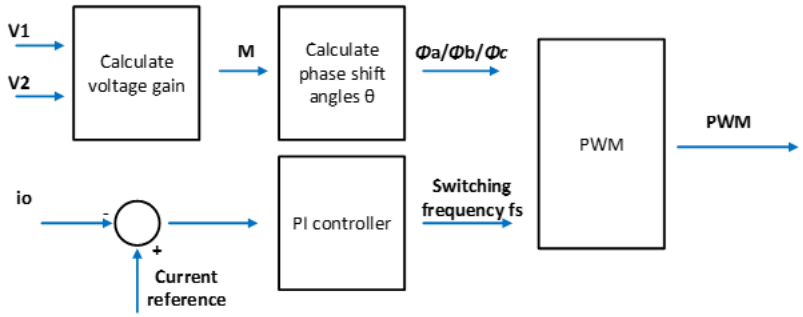


Figure 5-1. Control Block Diagram

Copyright © 2026 Texas Instruments Incorporated

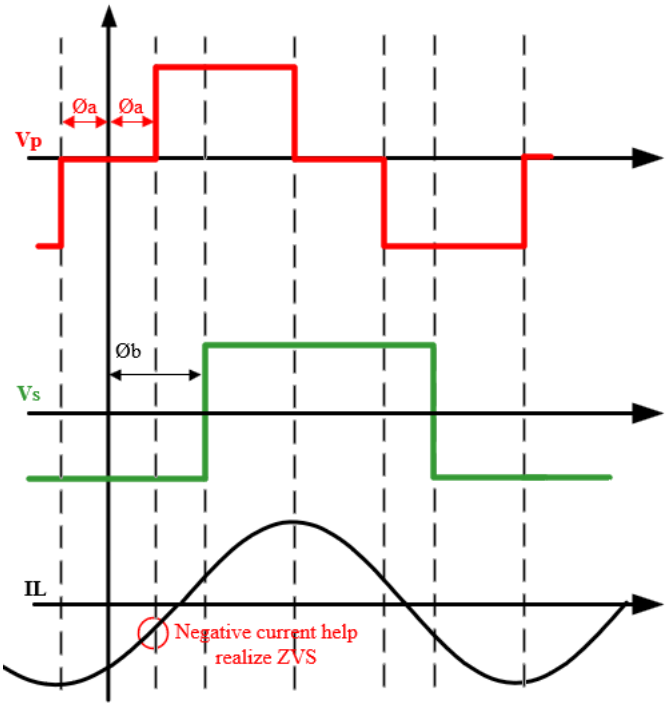


Figure 5-2. Operating Waveform with Negative Current to Help Realize ZVS

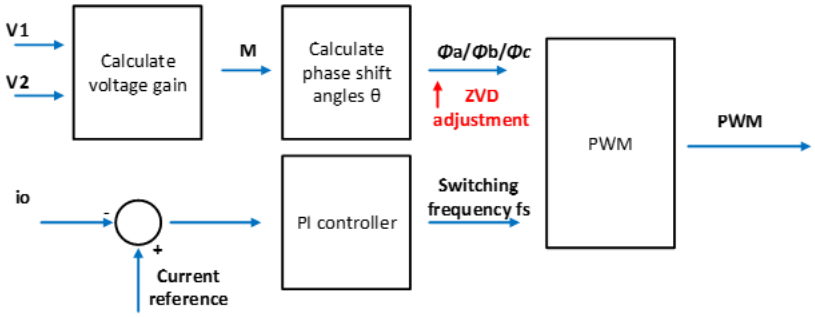


Figure 5-3. Control Block Diagram Combined With ZVD Function

Copyright © 2026 Texas Instruments Incorporated

6 Summary

To validate the proposed optimization modulation scheme, a 3.6kW SR-DAB converter is designed to charge and discharge a battery with a voltage variation of 40–60 VDC, the transformer ratio in this design is 8.33. Figure 6-1 shows the experimental efficiency curve under 400Vin, 40Vout and 52Vout. Figure 6-2 shows the operation waveforms at half load with 400Vin and 40Vout (that means M < 1) and the turn-off current is controlled at a low value. Figure 6-3 shows the waveforms at half load with 400Vin and 40Vout which uses the ZVD function of GaN in high voltage side. The high voltage side achieve ZVS while the turn-off current is controlled at a low value in the low voltage side.

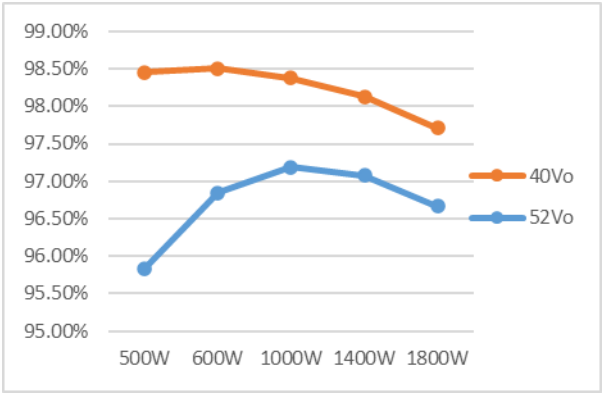


Figure 6-1. Efficiency Curve of SR-DAB

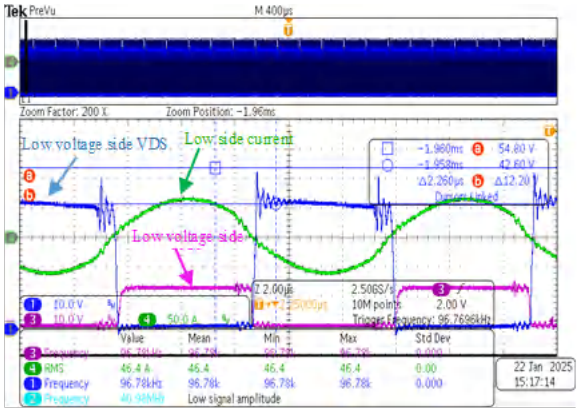


Figure 6-2. Experimental Waveform at 1800W

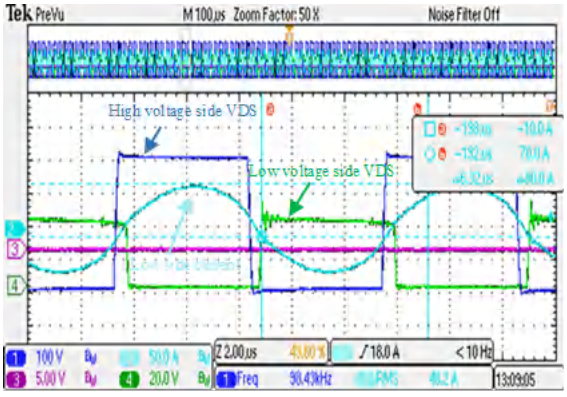


Figure 6-3. Experimental Waveform Combined With ZVD Function

Copyright © 2026 Texas Instruments Incorporated

7 References

1. T. Horiba, *Lithium-Ion Battery Systems* in Proceedings of the IEEE, vol. 102, no. 6, pp. 939-950, June 2014
2. Federal Consortium for Advanced Batteries, *Executive Summary - National Blueprint for Lithium Batteries 2021-2030*
3. Texas Instruments, *Designing an LLC resonant half-bridge power converter*, seminar.
4. Texas Instruments, *Designing a High-Power Bidirectional AD/DC Power Supply Using SiC FETs*, seminar.
5. X. Li and A. K. S. Bhat, "Analysis and Design of High-Frequency Isolated Dual-Bridge Series Resonant DC/DC Converter," in IEEE Transactions on Power Electronics, vol. 25, no. 4, pp. 850-862, April 2010.
6. A. F. Khan, S. S. Nag and B. Singh, "Analysis, Design, and Comparison of Isolated DC-DC Converters for Traction Application," *2023 IEEE Transportation Electrification Conference & Expo (ITEC)*, Detroit, MI, USA, 2023, pp. 1-6.

Copyright © 2026 Texas Instruments Incorporated

IMPORTANT NOTICE AND DISCLAIMER

TI PROVIDES TECHNICAL AND RELIABILITY DATA (INCLUDING DATASHEETS), DESIGN RESOURCES (INCLUDING REFERENCE DESIGNS), APPLICATION OR OTHER DESIGN ADVICE, WEB TOOLS, SAFETY INFORMATION, AND OTHER RESOURCES “AS IS” AND WITH ALL FAULTS, AND DISCLAIMS ALL WARRANTIES, EXPRESS AND IMPLIED, INCLUDING WITHOUT LIMITATION ANY IMPLIED WARRANTIES OF MERCHANTABILITY, FITNESS FOR A PARTICULAR PURPOSE OR NON-INFRINGEMENT OF THIRD PARTY INTELLECTUAL PROPERTY RIGHTS.

These resources are intended for skilled developers designing with TI products. You are solely responsible for (1) selecting the appropriate TI products for your application, (2) designing, validating and testing your application, and (3) ensuring your application meets applicable standards, and any other safety, security, regulatory or other requirements.

These resources are subject to change without notice. TI grants you permission to use these resources only for development of an application that uses the TI products described in the resource. Other reproduction and display of these resources is prohibited. No license is granted to any other TI intellectual property right or to any third party intellectual property right. TI disclaims responsibility for, and you fully indemnify TI and its representatives against any claims, damages, costs, losses, and liabilities arising out of your use of these resources.

TI’s products are provided subject to TI’s Terms of Sale, TI’s General Quality Guidelines, or other applicable terms available either on ti.com or provided in conjunction with such TI products. TI’s provision of these resources does not expand or otherwise alter TI’s applicable warranties or warranty disclaimers for TI products. Unless TI explicitly designates a product as custom or customer-specified, TI products are standard, catalog, general purpose devices.

TI objects to and rejects any additional or different terms you may propose.

Copyright © 2026, Texas Instruments Incorporated

Last updated 10/2025